

# Bone Piezoelectricity-Mimicking Nanocomposite Membranes Enhance Osteogenic Differentiation of Bone Marrow Mesenchymal Stem Cells by Amplifying Cell Adhesion and Actin Cytoskeleton

Xiaowen Sun<sup>1,2,3,†</sup>, Yunyang Bai<sup>3,†</sup>, Xiaona Zheng<sup>3</sup>, Xiaochan Li<sup>3</sup>, Yingying Zhou<sup>4</sup>, Yijun Wang<sup>4</sup>, Boon Chin Heng<sup>5,\*</sup>, and Xuehui Zhang<sup>1,6,\*</sup>

<sup>1</sup>Department of Dental Materials & Dental Medical Devices Testing Center, Peking University School and Hospital of Stomatology, Beijing, 100081, PR China

<sup>2</sup>Department of Prosthodontics, Peking University School and Hospital of Stomatology, Beijing, 100081, PR China

<sup>3</sup>Department of Geriatric Dentistry, Peking University School and Hospital of Stomatology, Beijing, 100081, PR China

<sup>4</sup>Department of Medical Technology, Peking University Health Science Center, Beijing, 100081, PR China

<sup>5</sup>Central Laboratory, Peking University School and Hospital of Stomatology, Beijing, 100081, PR China

<sup>6</sup>National Engineering Laboratory for Digital and Material Technology of Stomatology, NMPA Key Laboratory for Dental Materials, Beijing Laboratory of Biomedical Materials & Beijing Key Laboratory of Digital Stomatology, Peking University School and Hospital of Stomatology, Beijing, 100081, PR China

Ferroelectric biomaterials have been widely investigated and demonstrated to enhance osteogenesis by simulating the inherent electrical properties of bone tissues. Nevertheless, the underlying biological processes are still not well-understood. Hence, this study investigated the underlying biological processes by which bone piezoelectricity-mimicking barium titanate/poly(vinylidene fluoride-trifluoroethylene) nanocomposite membranes (BTO nanocomposite membranes) promote osteogenesis of Bone Marrow Mesenchymal Stem Cells (BMSCs). Our results revealed that the piezoelectric coefficient ( $d_{33}$ ) of nanocomposite membranes after controlled corona poling was similar to that of native bone, and exhibited highly-stable piezoelectrical properties and concentrated surface electrical potential. These nanocomposite membranes significantly enhanced the adhesion and spreading of BMSCs, which was manifested as increased number and area of mature focal adhesions. Furthermore, the nanocomposite membranes significantly promoted the expression of integrin receptors genes ( $\alpha1$ ,  $\alpha5$  and  $\beta3$ ), which in turn enhanced osteogenesis of BMSCs, as manifested by upregulated Alkaline Phosphatase (ALP) and Bone Morphogenetic Protein 2 (BMP2) expression levels. Further investigations found that the Focal Adhesion Kinase (FAK)-Extracellular Signal-Regulated Kinase 1/2 (ERK 1/2) signaling axis may be involved in the biological process of polarized nanocomposite membrane-induced osteogenesis. This study thus provides useful insights for better understanding of the biological processes by which piezoelectric or ferroelectric biomaterials promote osteogenesis.

**KEYWORDS:** Bone Piezoelectricity, Nanocomposite Membrane, Osteogenic Differentiation, FAK-ERK Signaling.

## INTRODUCTION

Biomimetic design has been shown to be a promising strategy to enhance the osteoinductive capacities

of a variety of materials [1–3]. The physical properties of natural bone, such as mechanics [4], electrical charges [5] and structural properties [6], provide meaningful cues for the design and improvement of implanted biomaterials. Electroactive biomaterials have attracted increasing attention in the biomaterial research field in recent years [7–10]. In particular, ferroelectric materials [11, 12] including polyvinylidene fluoride (PVDF),

\*Authors to whom correspondence should be addressed.  
Emails: hengboonchin@bjmu.edu.cn, zhangxuehui@bjmu.edu.cn  
†These two authors contributed equally to this work.  
Received: 21 March 2021  
Accepted: 27 April 2021

poly(vinylidene fluoride-trifluoroethylene) (P(VDF-TrFE)) and barium titanate ( $\text{BaTiO}_3$ , BTO), have been investigated as potential biomimetic materials that can simulate the piezoelectric properties of natural bone tissue [13–16].

Stem cell function (e.g., cell adhesion, spreading, proliferation and differentiation) can be directly regulated by biomaterial properties [17–20]. Understanding the biological processes of stem cell responses to biomechanical stimuli emanating from material physical properties, is essential for optimizing scaffold implant design and improving the biological functions of implant materials [21–24]. In previous studies by other research groups, a variety of electroactive materials have been demonstrated to effectively promote the adhesion [25, 26], proliferation [27–29] and osteogenesis [30, 31] of mesenchymal stem cells. In our previous study, biomimetic piezoelectric nanocomposite membrane containing barium titanate nanoparticles (BTO NPs) filler and P(VDF-TrFE) matrix had been demonstrated to enhance the osteogenic differentiation potential of BMSCs due to its inherent piezoelectric properties that mimic natural bone tissue [15, 16]. However, the underlying biological processes by which osteogenic differentiation of BMSCs is enhanced by surface electrical stimuli are still not well-understood.

Cells exhibit changes in adhesion and morphology under the influence of scaffold material properties [32–34]. Studies have shown that electrical stimuli can exert a profound effect on cell adhesion and cytoskeletal reorganization, as well as integrin expression [35, 36]. In our previous studies, the BMSCs spreading area, as well as individual focal adhesion area were significantly enhanced upon culture on the polarized BTO nanocomposite membrane surface [15]. Observed changes in cell spreading, skeletal reorganization and focal adhesion formation are directly related to cell mechanotransduction [37]. Previous studies have confirmed that the FAK-ERK signaling axis plays an important role in mediating cell mechanotransduction [38, 39]. Therefore, we hypothesize that FAK-ERK signaling may be implicated in the biological process by which surface electrical stimuli from biomimetic ferroelectric BTO nanocomposite membranes promote osteogenic differentiation of BMSCs.

Therefore, this study sought to investigate the underlying biological processes by which biomimetic ferroelectric BTO nanocomposite membranes promote osteogenic differentiation of BMSCs. The biological functions of cultured BMSCs on the polarized composite membrane was characterized, including cell adhesion, spreading, cytoskeletal organization, integrin expression and osteogenic differentiation, in comparison with unpolarized nanocomposite membranes. Additionally, the biological process by which mechanotransduction mediated by integrin receptors lead to activation of intracellular signaling pathways including FAK-ERK, was also explored.

## EXPERIMENTAL DETAILS

### Preparation of Biomimetic Piezoelectric BTO Nanocomposite Membranes

BTO nanocomposite membranes were fabricated as documented in our previous research [15]. Briefly, the dopamine-modified BTO NPs were mixed with P(VDF-TrFE) solution, in which co-polymer powders were dissolved in *N,N*-dimethylformamide (DMF) at 5% vol. After stirring, a stable suspension was formed which was cast into membranes. The polarized BTO nanocomposite membranes were fabricated by corona discharge under a 1 kV/mm DC field at room temperature for 30 min duration.

### Characterization of the Biomimetic Piezoelectric BTO Nanocomposite Membrane

Field Emission Scanning Electron Microscopy (FE-SEM, HITACHI, S-4800) and Energy Dispersion Spectroscopy (EDS, Japan) were used to evaluate the morphology and elemental composition of unpolarized and polarized BTO nanocomposite membrane respectively. The surface roughness of BTO nanocomposite membranes was characterized by Atomic Force Microscopy (AFM, Bruker) under contact mode. Water contact angle measurement was used to evaluate surface wettability of the membranes by using the video contact angle instrument (JC2000C1, China). The universal mechanical testing machine (INSTRON-1121) was used to measure elastic moduli of the nanocomposite membranes. The polarization-electric field loop (P-E) and piezoelectric coefficient ( $d_{33}$ ) were measured by using the ferroelectric analyzer (TF1000, aixACCT) and the piezoelectric coefficient meter (ZJ-3AN, IACAS) respectively. Scanning Kelvin Probe Microscopy (SKPM) (Multimode8, Bruker Co, USA) was used to measure the surface electrical potential.

### BMSCs Adhesion on the Biomimetic Piezoelectric Nanocomposite Membrane

Rat BMSCs (Cyagen, Guangzhou, China) were cultivated in Dulbecco's Modified Eagle's Medium (DMEM) with Fetal Bovine Serum (FBS) at 10% (v/v) and penicillin-streptomycin at 1% (v/v). BMSCs ( $3 \times 10^4$  cells/well) were cultured on the two types of composite membranes in a 12-well plate for 6 h. Subsequently, the samples were fixed and permeabilized, then stained with either anti-vinculin (ab129002, Abcam, diluted 1:250) or anti-integrin alpha 5 (ab150361, Abcam, diluted 1:250) primary antibody. After washing and incubation with the secondary antibody (ab150077, Abcam, diluted 1:1000), the samples were stained for F-actin and nuclear DNA. The images were then captured under confocal laser scanning microscopy (SP8, Leica). Semi-quantitative analysis was performed by using the LAS X software. The expression of *Itga1*, *Itga5* and *Itgb3* mRNA transcripts in BMSCs after 6 h of culture were detected by Quantitative Real-Time PCR. Each

experiment had three replicates. The primer sequences of integrin-related genes are listed in Table I.

### Osteogenic Differentiation of BMSCs on Biomimetic Piezoelectric Nanocomposite Membranes

BMSCs ( $3 \times 10^4$  cells/well) were cultured on unpolarized and polarized biomimetic nanocomposite membranes within a 12-well plate. After 3 days of culture, RUNX2 and BMP2 expression were detected through immunocytochemistry. The samples were stained with primary antibodies against RUNX2 (ab23981, Abcam, diluted 1:250) or BMP2 (ab214821, Abcam, diluted 1:250) at 4 °C. After removal of excess antibodies, the samples were stained with secondary antibody (ab150077, Abcam, diluted 1:1000) at room temperature. The fluorescently-labeled samples were observed under SP8, and the mean fluorescence intensities were analyzed using the LAS X software, with at least 20 cells in each group.

BMSCs ( $4 \times 10^4$  cells/well) were seeded on BTO nanocomposite membranes within 12-well plates and cultured for 1, 3 and 7 days. The expression levels of BMP2, ALP, Runt-related Transcription Factor 2 (RUNX2), Osteopontin (OPN) and Collagen Type 1 alpha 1 (Col1a1) were analyzed by RT-qPCR, based on manufacturer's recommended protocol. All experiments were carried out with three replicates. The primer sequences of osteogenic genes are listed in Table I.

### Analyzing the Biological Process of BMSCs Osteogenic Differentiation

The BMSCs ( $2 \times 10^5$  cells/well) were cultured on unpolarized and polarized composite membranes within 6-well plates for 6 h. Then the integrin  $\alpha 5\beta 1$  antagonist ANT-161 trifluoroacetate salt was used to treat BMSCs at a working concentration of 1  $\mu$ M. The total cellular protein was resolved by electrophoresis and electrotransferred to PVDF membranes, then the membranes were blocked with 5% (w/v) Difco Skimmed Milk (BD, USA) at ambient temperature, prior to being incubated overnight at 4 °C with Itg $\alpha 5$ , Focal Adhesion Kinase (FAK), phospho-Focal Adhesion Kinase (p-FAK), ERK 1/2, phospho-ERK 1/2

(p-ERK 1/2), RUNX2, BMP2 and GAPDH primary antibodies respectively. After thorough washing with TBST, the horseradish peroxidase (HRP)-conjugated anti-rabbit IgG and anti-mouse IgG(H+L) secondary antibodies were used to detect the bound primary antibodies at room temperature. The stained images of PVDF membranes were visualized with an ECL chemiluminescence reagent (CW BIO, Jiangsu, China).

### Statistical Analysis

Quantitative results were depicted as mean  $\pm$  standard error of mean (SEM). The SPSS 19.0 software (IBM) was used to carry out statistical analysis and differences between independent samples were analyzed with the Student's *t*-test. The threshold of statistical significance was assigned at \**p* < 0.05, with \*\**p* < 0.01 being considered very significant and \*\*\**p* < 0.001 being considered highly significant.

## RESULTS AND DISCUSSION

### Physico-Chemical Properties of the BTO Nanocomposite Membrane

It can be observed from FE-SEM images that surface morphology of nanocomposite membranes remain unaltered by polarization treatment (Fig. 1(a)). The presence of BTO NPs within membrane matrix was detected through EDS spectra (Fig. 1(a)). AFM analysis indicated that all fabricated membranes, either the unpolarized or polarized membranes displayed nanoscale surface roughness (Fig. 1(b)). The quantitative data suggested that there were no significant differences in surface roughness (Fig. 1(f)), water contact angle (Fig. 1(d)) and elastic moduli (Fig. 1(e)) between the unpolarized and polarized membranes.

The electrical properties of the polarized BTO nanocomposite membranes were further characterized. Polarization-electric field loops (P-E) (Fig. 1(g)) validated the ferroelectric nature of BTO nanocomposite membranes. After corona poling treatment, maximal polarization ( $P_m$ ) and residual polarization ( $P_r$ ) were observed to increase. Due to electrical polarization, there was substantially increased surface electric potential with a high-potential pitting distribution on the polarized BTO composite membranes,

**Table I.** Primers sequences for cell adhesion and osteogenic differentiation in BMSCs on biomimetic piezoelectric BTO nanocomposite membranes.

Target gene	Forward primer sequence (5'–3')	Reverse primer sequence (5'–3')
<i>Itg<math>\alpha 1</math></i>	TGATGACGCTCTGCCAACT	CACCACTGTCCTGGTGTGGT
<i>Itg<math>\alpha 5</math></i>	TACCTGGGTGACAAGAACGC	CTGGTTCACCGCAAGTAGT
<i>Itg<math>\beta 3</math></i>	CCACTGATGCCAAGACCCAT	AGGCTGACGACATTTTCGGT
<i>RUNX2</i>	CAGTATGAGAGTAGGTGTCCCGC	AAGAGGGGTAAGACTGGTCATAGG
<i>BMP2</i>	ACAAACGAGAAAAGCGTCAAGC	CCCACATCACTGAAGTCCACATA
<i>ALP</i>	AGTGGTATTGTAGGTGCTGTGGT	AGAGTGACGGTGTCTAGCCT
<i>OPN</i>	GATGAACAGTATCCCGATGCC	CCCTCTGCTTATACTCCTTGGAC
<i>Col1a1</i>	CAGATTGAGAACATCCGCAGC	CGGAACCTTCGCTCCATACTC
<i>GAPDHA</i>	GTGCCAGCCTCGTCTCATA	GATGGTGTGGGTTTCCCGT

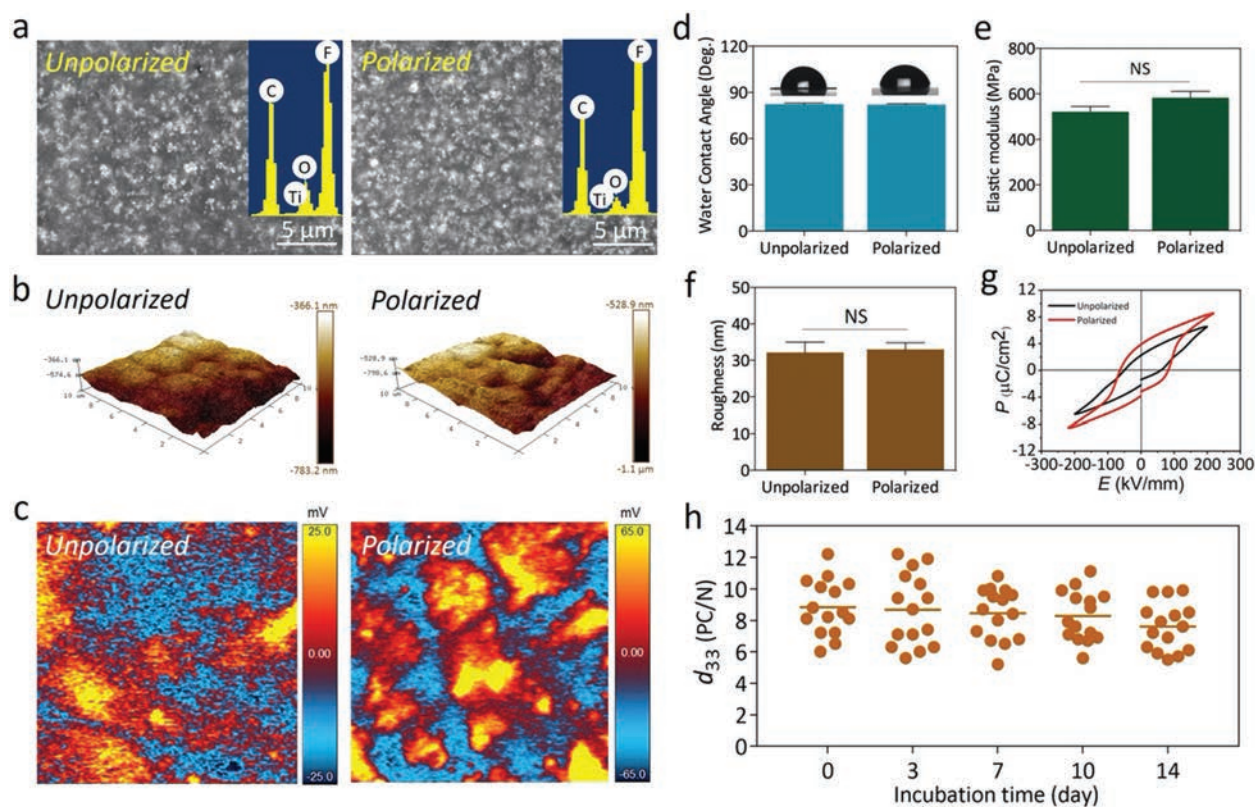


**Figure 1.** Characterization of BTO nanocomposite membrane. (a) Representative SEM images of surface morphologies of the nanocomposite membrane before and after corona poling treatment. Insets are the EDS spectras. (b) Representative AFM images of composite membranes before and after corona poling treatment. (c) Surface potential images of unpolarized and polarized composite membranes. (d) Water contact angles of the membranes before and after corona poling treatment. (e) Elastic moduli of unpolarized and polarized composite membranes. (f) The quantitative analysis of the surface roughness of composite membranes. (g) The hysteresis loops of unpolarized and polarized nanocomposite membranes. (h) The piezoelectric coefficient ( $d_{33}$ ) values of the polarized membranes after immersing for different time durations in serum-free cell culture medium. NS: No significant.

**Abbreviations:** P(VDF-TrFE), poly(vinylidene fluoride-trifluoroethylene); SEM, Scanning electron microscopy; EDS, Energy disperse spectroscopy; AFM, Atomic force microscope.

while the unpolarized nanocomposite membrane surface had a much lesser concentration of surface electric potential (Fig. 1(c)). The concentrated surface electric potential on polarized BTO nanocomposite membranes is due to enhanced interfacial polarization between BTO NPs and P(VDF-TrFE) after polarization treatment [40].

Additionally, the piezoelectric coefficient of polarized BTO composite membrane was analyzed to evaluate its inverse piezoelectric effect. It was found that the piezoelectric coefficient ( $d_{33}$ ) of the membrane ( $\sim 8.82$  pC/N) was similar to that of native bone and remained stable at about 86% of its original value, even after 14 days of simulated physiological conditions (Fig. 1(h)). The high stability of the piezoelectric coefficient is likely due to the high residual polarization of BTO composite membranes, as explained by large interface polarization between BTO nanoparticles with a high specific surface area and P(VDF-TrFE) matrix [15–41]. Taken together, the polarized nanocomposite membrane can be utilized as a material model for studying the biological processes

by which polarized surface charge stimulation promote osteogenic differentiation of BMSCs, excluding the influence of other physical and chemical properties [42].

### Biomimetic Piezoelectric BTO Nanocomposite Membrane Promotes BMSCs Adhesion and Cytoskeletal Reorganization

Cell adhesion and morphological changes are the primary manifestations of cellular response to material properties. As shown in Figure 2, BMSCs prominently displayed polygonal osteoblastic-like cell morphology with prominent filopodia on polarized BTO nanocomposite membranes after culturing for 6 h, whereas BMSCs cultured on the unpolarized composite membranes displayed less filopodia and lamellipodia formation (Fig. 2(a)). This thus indicated that polarized nanocomposite membranes enhanced BMSCs adhesion and spreading. Filopodia is thought to act as guiding cues for cell elongation and polygonal-like shape, with the focal adhesion (FA) complex being formed right behind along the filopodia

axis [43]. Therefore, we further investigated and confirmed that there was enhanced FA formation by BMSCs cultured on the polarized nanocomposite membrane, as demonstrated by immunostaining for vinculin expression after 6 h of culture (Fig. 2(b)). Quantitative analysis revealed that the cell spreading area, the number and area of FAs on the polarized nanocomposite membrane were significantly larger than those of the unpolarized

membrane (Figs. 2(d–f)). Consistent with previous related studies, cells with increased spreading area and polygonal shape suggested stronger adhesion [44, 45]. As described in previous studies, cells react to biophysical signals of the extracellular microenvironment via integrin-based adhesion sites [46]. We hereby speculate that focal adhesion complexes are involved in the transduction of polarized surface charge stimulation signal into the F-actin

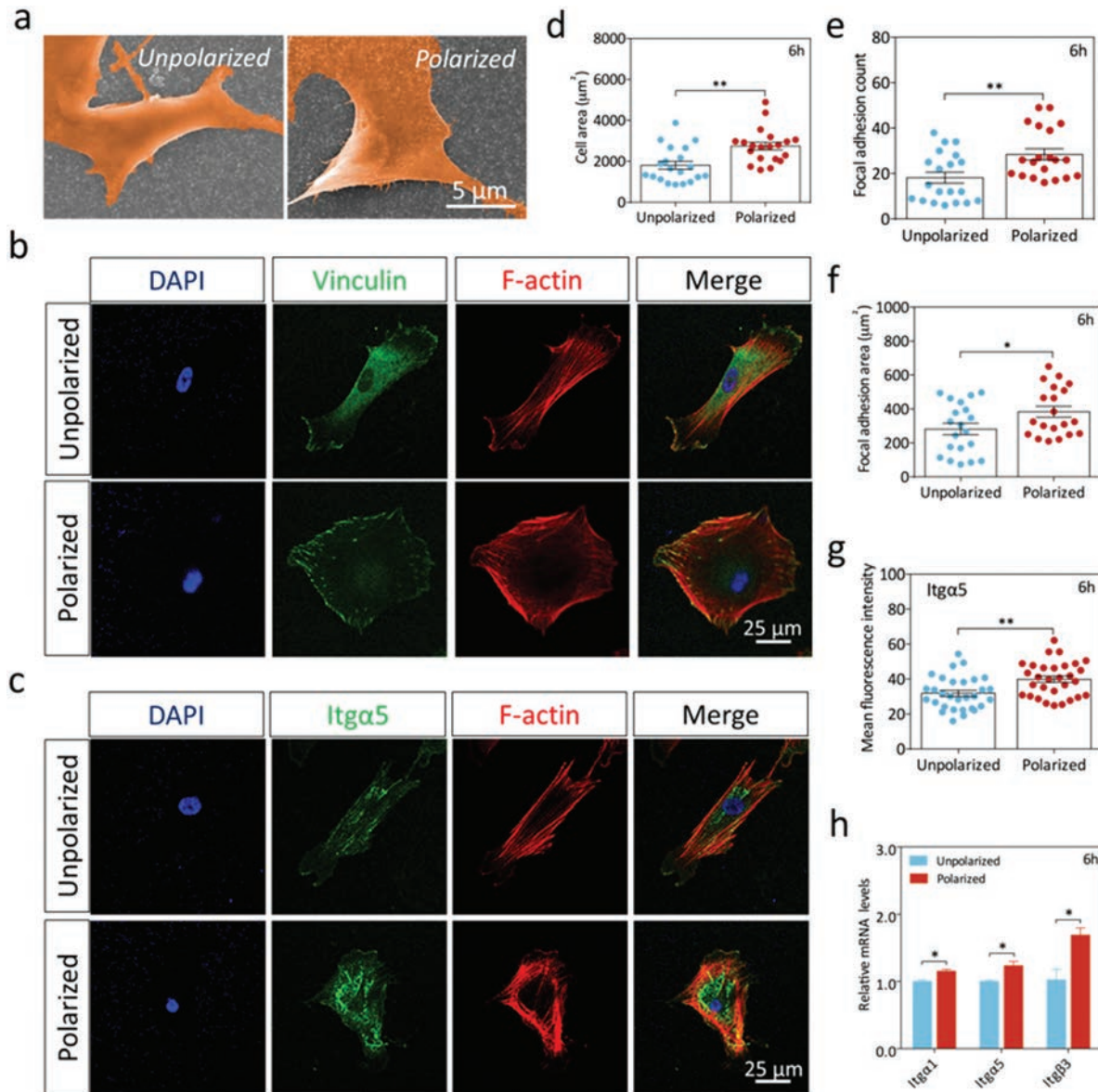


**Figure 2.** BMSCs morphology and adhesion on biomimetic piezoelectric BTO nanocomposite membranes. (a) Representative SEM images showing the morphology and spreading of BMSCs on the polarized versus unpolarized membrane; (b) Representative immunofluorescence images to visualize the expression of Vinculin (green), F-actin (red) by BMSCs after 6 h of culture, with cell nuclei being stained with DAPI (blue); (c) Representative immunofluorescence images to visualize the expression of Itga5 (green), F-actin (red), and nuclei (blue) by BMSCs after 6 h of culture on the nanocomposite membranes; (d) Quantification of the cell spreading area of BMSCs. (e) Quantification of the focal adhesion count of BMSCs. (f) Quantification of the focal adhesion area of BMSCs. (g) Quantification of the mean fluorescence intensity of Itga5. (h) RT-qPCR analysis of the gene expression levels of integrin subunits (Itga1, Itga5 and Itgb3) after 6 h of culture. (\* $p < 0.05$ , \*\* $p < 0.01$ ).

**Abbreviations:** RT-qPCR, Reverse transcription-quantitative polymerase chain reaction; Itga1, Integrin alpha 1; Itga5, Integrin alpha 5; Itgb3, Integrin beta 3.

cytoskeleton, thereby activating the expression of related functional genes.

Focal adhesion assembly depends on the type of engaged integrin. After culture for 6 h, *Itga5* expression was enriched on polarized membranes with the highest mean fluorescence intensity (Figs. 2(c and g)), as

compared to unpolarized membranes. Furthermore, the polarized membranes induced a higher gene expression level of integrin subunits, such as *Itga1*, *Itga5*, and *Itgb3* in BMSCs after 6 h culture, in comparison to the unpolarized samples (Fig. 2(h)). The upregulated expression of integrin subunits may be attributed to increased

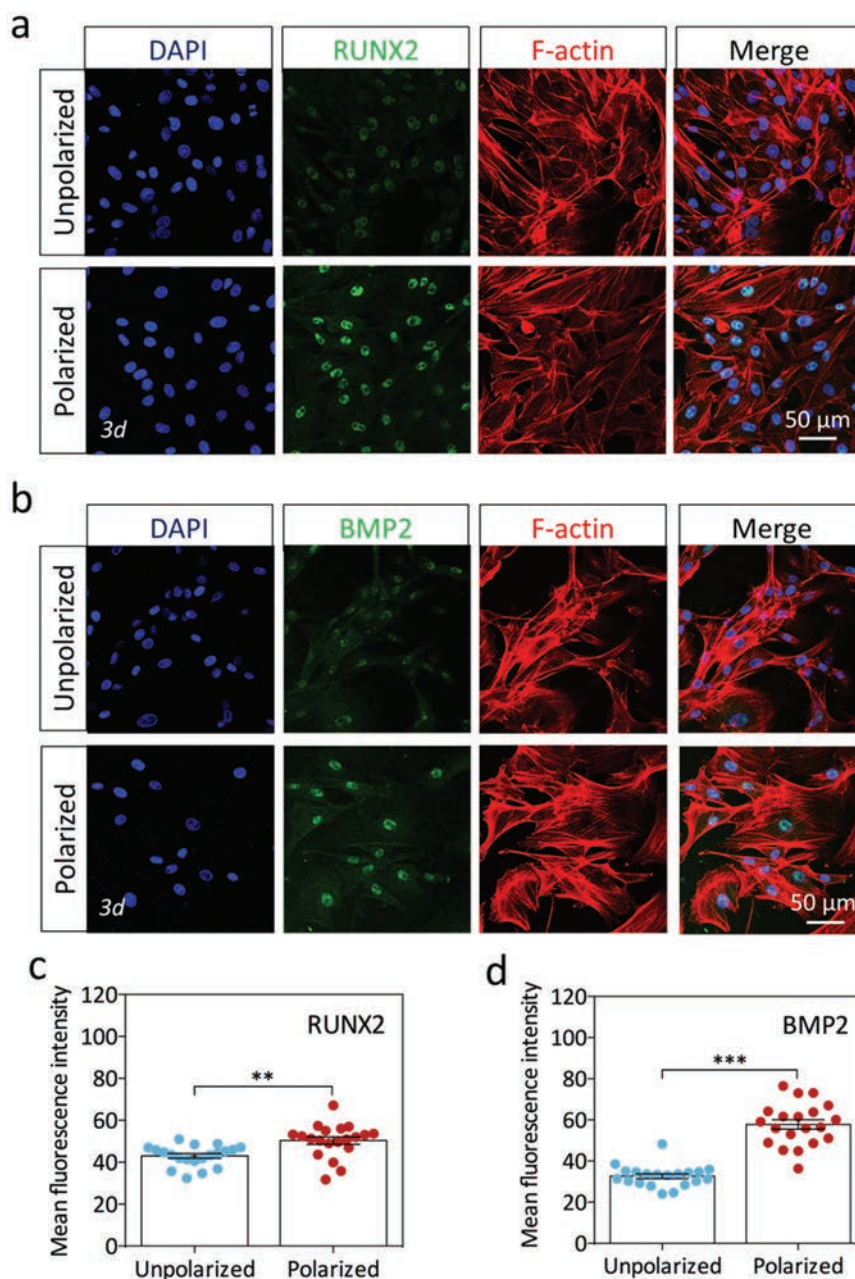


**Figure 3.** Osteogenic differentiation of BMSCs on biomimetic piezoelectric BTO nanocomposite membranes. (a) Representative immunofluorescence images for visualizing the expression of RUNX2 (green), F-actin (red), and cell nuclei (blue) in BMSCs after 3 days of culture. (b) Representative immunofluorescence images for visualizing the expression of BMP2 (green), F-actin (red), and cell nuclei (blue) after 3 days of culture on the nanocomposite membranes. (c) Quantification of the mean fluorescence intensity of RUNX2. (d) Quantification of the mean fluorescence intensity of BMP2. Error bars represent standard error. (\*\* $p < 0.01$ , \*\*\* $p < 0.001$ ).

**Abbreviations:** BMSCs, Bone marrow mesenchymal stem cells; RUNX2, Runt-related transcription factor 2; BMP2, Bone morphogenetic protein 2; F-actin, actin cytoskeleton.

cytoskeletal organization, enhanced cell spreading and increased focal adhesion formation induced by surface charge stimuli emanating from the polarized membranes, as previously mentioned. Integrin plays a crucial role during the mechanotransduction process and transmission of biomechanical stimuli across integrin-based focal adhesions triggered changes in gene expression and induced rapid responses via associated signaling cascades [46]. Overall, these results implied that biomimetic surface electrical stimuli emanating from the polarized nanocomposite membrane may activate integrin-dependent cell adhesion to promote BMSCs activity and function.

### Biomimetic Piezoelectric BTO Nanocomposite Membrane Promotes BMSCs Osteogenic Differentiation

There is increasing evidence that integrin-mediated cellular processes play key roles in osteogenesis [47]. Therefore, we further investigated the osteogenic differentiation of BMSCs on the nanocomposites membranes without osteogenic supplements. According to previous studies, RUNX2 and BMP2 are usually selected as the osteogenic markers of BMSCs [48, 49]. Immunocytochemistry showed that BMSCs were markedly enriched in RUNX2 (Fig. 3(a)) and BMP2 (Fig. 3(b)) expression after culturing for 3 days on polarized composite membranes, which was also validated by quantitative analysis (Figs. 3(c and d)). Then, we analyzed the osteogenic-related gene expression levels of BMSCs on the unpolarized and polarized membranes. The osteogenic gene markers RUNX2 and BMP2 were obviously up-regulated after 1 day of culture (Fig. 4(a)), RUNX2, BMP2 and ALP were up-regulated after 3 days of culture (Fig. 4(b)), while OPN and Col1a1 were up-regulated after 7 days of culture on the polarized nanocomposite membranes (Fig. 4(c)). These

results thus suggest that biomimetic piezoelectric membranes possess good osteoinductivity, which is consistent with our previous studies [15–50]. Additionally, the results presented in this study were also consistent with the scientific literature, in which charged materials promoted the expression of osteogenic markers in bone marrow mesenchymal stem cells [51, 52]. The enhanced osteogenic differentiation results were likely due to persistent polarization arising from residual polarization of ferroelectric biomaterials after corona poling treatment, as reported previously by our research group [15–54]. These results may imply that the polarized surface charge stimuli emanating from the polarized BTO nanocomposite membrane exhibits its potent osteoinductive function through the promotion of integrin-mediated cell adhesion and focal adhesion formation.

### The Mechanotransduction Process of Biomimetic Piezoelectric Nanocomposite Membrane-Induced Osteogenesis

In order to elucidate how biomimetic piezoelectric stimuli are transduced into intracellular biological signals via integrin receptors to activate osteogenesis of BMSCs, we investigated the Itg-FAK-ERK signaling axis. As depicted in Figure 5, after 6 hours of culture, the polarized BTO nanocomposite membranes induced a significant increase of phosphorylated ERK 1/2 (p-ERK1/2), which indicated activation of ERK signaling (Fig. 5(a)). Meanwhile, the relative staining intensities of Itga5 and p-FAK expression in BMSCs cultured on polarized membranes were higher than those of the unpolarized membranes (Fig. 5(a)). The expression of osteogenic-related markers RUNX2 and BMP2 were enhanced on polarized membranes (Fig. 5(a)). To investigate the roles of integrin receptors and Itg-FAK-ERK signaling in mediating the transduction of electrical

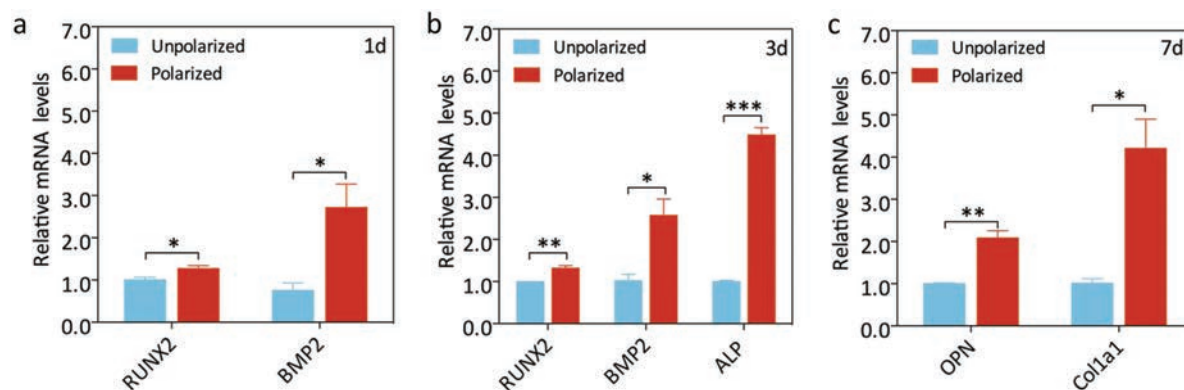


**Figure 4.** Osteogenic differentiation-related gene expressions by BMSCs cultured on biomimetic piezoelectric BTO nanocomposite membranes. (a) RT-qPCR analysis of the gene expression levels of RUNX2 and BMP2 by BMSCs cultured for 1 day on the nanocomposite membranes; (b) RT-qPCR analysis of the gene expression levels of RUNX2, BMP2 and ALP by BMSCs cultured for 3 days on the nanocomposite membranes; (c) RT-qPCR analysis of the gene expression levels of OPN and Col1a1 by BMSCs cultured for 7 days on the nanocomposite membranes. Results were standardized using GAPDH as the housekeeping gene, and are presented as relative mRNA levels. (\* $p < 0.05$ , \*\* $p < 0.01$ , \*\*\* $p < 0.001$ ).

**Abbreviations:** ALP, alkaline phosphatase; OPN, osteopontin; Col1a1, collagen type 1 alpha 1.

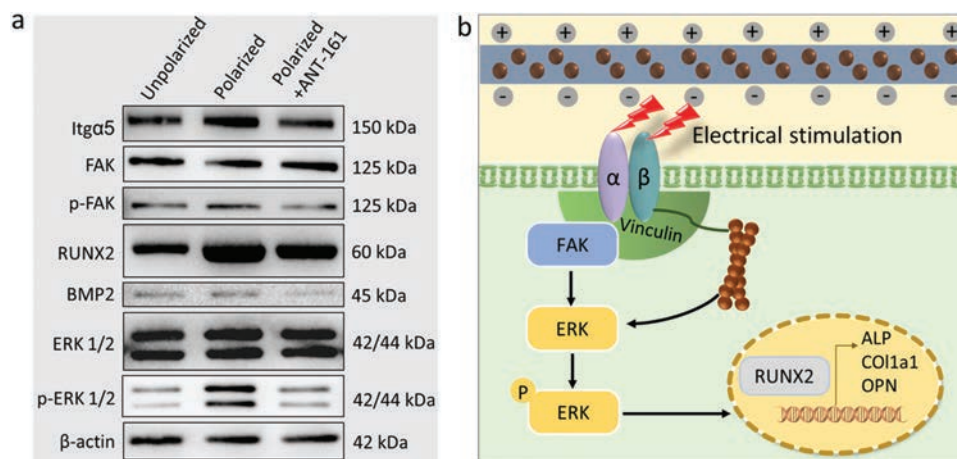


**Figure 5.** The mechanotransduction process of biomimetic piezoelectric BTO nanocomposite membrane-induced osteogenesis. (a) Western Blot analysis of the expression of Itg $\alpha$ 5, FAK, p-FAK, RUNX2, BMP2, ERK 1/2 and p-ERK 1/2 in BMSCs cultured for 6 h on nanocomposite membranes without and with inhibitor ANT-161. (b) Schematic illustration of the ERK signaling pathway and its proposed involvement in biomimetic polarized surface charge-mediated osteogenic differentiation of BMSCs.

**Abbreviations:** FAK, Focal Adhesion Kinase; p-FAK, phospho-Focal Adhesion Kinase; ERK 1/2, Extracellular Signal-Regulated Kinases 1/2; p-ERK 1/2, phospho-Extracellular Signal-Regulated Kinases 1/2.

stimuli into pro-osteogenic intracellular signaling cues within BMSCs, the integrin  $\alpha$ 5 $\beta$ 1 antagonist ANT-161 was added to inhibit expression of Itg $\alpha$ 5 in BMSCs cultured on polarized nanocomposite membranes, which was accompanied with downregulated expression of RUNX2 and BMP2. Additionally, marked reduction of p-ERK1/2 and p-FAK expression levels were accompanied by inhibition of Itg $\alpha$ 5 (Fig. 5(a)).

We thus confirmed the key role of Itg-FAK-ERK1/2 signaling in transducing electrical stimuli from biomimetic piezoelectric membranes into intracellular signaling cues that activated osteogenesis of BMSCs. ERK1/2 is an important transcription factor in the mechanotransduction process, which upon phosphorylation triggered RUNX2 mediated osteogenesis [55, 56]. We hypothesized that mechanosensing of electrical stimuli from the polarized BTO nanocomposite membranes was transduced via the Itg-FAK-ERK1/2 axis into pro-osteogenic signaling cues within the nuclei of BMSCs, thereby regulating the osteogenesis of BMSCs [57, 58]. The experimental observations were consistent with this hypothesis, with the polarized membranes inducing a significant increase in the protein expression levels of Itg $\alpha$ 5, p-FAK and p-ERK 1/2, as well as the osteogenic markers RUNX2 and BMP2. Upon treatment with the integrin  $\alpha$ 5 $\beta$ 1 antagonist ANT-161 [59], attenuated expression of Itg $\alpha$ 5 in BMSCs cultured on polarized membranes was accompanied with significantly decreased expression of p-FAK, RUNX2, BMP2 and p-ERK 1/2 (Fig. 5(a)). A schematic depiction of how Itg-FAK-ERK signaling mediate transduction of electrical stimuli from the biomimetic piezoelectric membranes into intracellular signaling cues that activate osteogenic differentiation of BMSCs is illustrated in Figure 5(b). Our results thus explain the biological process

by which piezoelectric stimuli activates membrane-bound integrin, such as Itg $\alpha$ 5, which in turn leads to increased cell adhesion, and initiation of downstream mechanotransduction via FAK and ERK 1/2 signaling, subsequently upregulating other transcription factors to promote osteogenesis of BMSCs.

In summary, these findings show that the biomimetic piezoelectric BTO nanocomposite membrane has favorable physico-chemical and mechanical properties that meet the clinical application requirements for barrier membranes developed to guide tissue regeneration. More importantly, this study delineates the biological process of how osteogenic differentiation of BMSCs is enhanced by surface charge generated by residual polarization of materials, which in turn lays the foundation for optimizing the osteoinductive properties of conventional guided tissue regeneration membranes.

## CONCLUSIONS

This study demonstrates that biomimetic surface charge stimuli emanating from polarized BTO nanocomposite membranes could activate integrin-dependent cell adhesion to promote BMSCs activity and function. Further investigations found that FAK-ERK signaling may be involved in the biological process of polarized nanocomposite membrane-induced osteogenesis. Consequently, we infer that the enhancement of osteogenesis by polarized BTO nanocomposite membranes is actually a process of transforming physical signals from extracellular polarized surface charge stimuli into intracellular mechanotransduction signaling cues. Our results thus provide useful information that deepen our understanding of the underlying biological processes by which surface electrical stimuli

from electroactive materials are converted into biological signals that regulate osteogenic differentiation of stem cells.

### Conflicts of Interest

The authors declare no conflicts of interest.

**Acknowledgments:** This work was supported by the National Key R&D Program of China (Nos. 2018YFC1105303/04), National Natural Science Foundation of China (Nos. 82022016, 51772006, 51973004), Beijing Municipal Science & Technology Commission Projects (No. Z181100002018001), and Peking University Medicine Fund (PKU2020LCXQ009). All co-authors hereby declare no conflicts of interest in this study.

### REFERENCES

- Wang, H.Y. and Heilshorn, S.C., **2015**. Adaptable hydrogel networks with reversible linkages for tissue engineering. *Advanced Materials*, 27(25), pp.3717–3736.
- Shih, Y.R.V., Hwang, Y., Phadke, A., Kang, H., Hwang, N.S., Caro, E.J., Nguyen, S., Siu, M., Theodorakis, E.A., Gianneschi, N.C., Vecchio, K.S., Chien, S., Lee, O.K. and Varghese, S., **2014**. Calcium phosphate-bearing matrices induce osteogenic differentiation of stem cells through adenosine signaling. *Proceedings of the National Academy of Sciences of the United States of America*, 111(3), pp.990–995.
- Holzwarth, J.M. and Ma, P.X., **2011**. Biomimetic nanofibrous scaffolds for bone tissue engineering. *Biomaterials*, 32(36), pp.9622–9629.
- Barthelat, F., Yin, Z. and Buehler, M.J., **2016**. Structure and mechanics of interfaces in biological materials. *Nature Reviews Materials*, 1(4), pp.1–16.
- Khare, D., Basu, B. and Dubey, A.K., **2020**. Electrical stimulation and piezoelectric biomaterials for bone tissue engineering applications. *Biomaterials*, 258, pp.1–25.
- Wegst, U.G.K., Bai, H., Saiz, E., Tomsia, A.P. and Ritchie, R.O., **2015**. Bioinspired structural materials. *Nature Materials*, 14(1), pp.23–36.
- Li, J., Wong, W.Y. and Tao, X.M., **2020**. Recent advances in soft functional materials: Preparation, functions and applications. *Nanoscale*, 12(3), pp.1281–1306.
- Jiang, W., Li, H., Liu, Z., Li, Z., Tian, J.J., Shi, B.J., Zou, Y., Ouyang, H., Zhao, C.C., Zhao, L.M., Sun, R., Zheng, H.R., Fan, Y.B., Wang, Z.L. and Li, Z., **2018**. Fully bioabsorbable natural-materials-based triboelectric nanogenerators. *Advanced Materials*, 30(32), pp.1–10.
- Guo, B.L. and Ma, P.X., **2018**. Conducting polymers for tissue engineering. *Biomacromolecules*, 19(6), pp.1764–1782.
- Feiner, R. and Dvir, T., **2018**. Tissue-electronics interfaces: From implantable devices to engineered tissues. *Nature Reviews Materials*, 3(1), pp.1–16.
- Blazquez-Castro, A., Garcia-Cabanes, A. and Carrascosa, M., **2018**. Biological applications of ferroelectric materials. *Applied Physics Reviews*, 5(4), pp.1–19.
- Ribeiro, C., Sencadas, V., Correia, D.M. and Lanceros-Mendez, S., **2015**. Piezoelectric polymers as biomaterials for tissue engineering applications. *Colloids and Surfaces B-Biointerfaces*, 136, pp.46–55.
- Shuai, C.J., Zeng, Z.C., Yang, Y.W., Qi, F.W., Peng, S.P., Yang, W.J., He, C.X., Wang, G.Y. and Qian, G.W., **2020**. Graphene oxide assists polyvinylidene fluoride scaffold to reconstruct electrical microenvironment of bone tissue. *Materials & Design*, 190, pp.1–10.
- Shuai, C.J., Liu, G.F., Yang, Y.W., Yang, W.J., He, C.X., Wang, G.Y., Liu, Z., Qi, F.W. and Peng, S.P., **2020**. Functionalized BaTiO<sub>3</sub> enhances piezoelectric effect towards cell response of bone scaffold. *Colloids and Surfaces B-Biointerfaces*, 185, pp.1–10.
- Zhang, X., Zhang, C., Lin, Y., Hu, P., Shen, Y., Wang, K., Meng, S., Chai, Y., Dai, X., Liu, X., Liu, Y., Mo, X., Cao, C., Li, S., Deng, X. and Chen, L., **2016**. Nanocomposite membranes enhance bone regeneration through restoring physiological electric microenvironment. *ACS Nano*, 10(8), pp.7279–86.
- Bai, Y., Dai, X., Yin, Y., Wang, J., Sun, X., Liang, W., Li, Y., Deng, X. and Zhang, X., **2019**. Biomimetic piezoelectric nanocomposite membranes synergistically enhance osteogenesis of deproteinized bovine bone grafts. *International Journal of Nanomedicine*, 14, pp.3015–3026.
- Li, Y.L., Xiao, Y. and Liu, C.S., **2017**. The horizon of materiobiology: A perspective on material-guided cell behaviors and tissue engineering. *Chemical Reviews*, 117(5), pp.4376–4421.
- Wu, S.L., Liu, X.M., Yeung, K.W.K., Liu, C.S. and Yang, X.J., **2014**. Biomimetic porous scaffolds for bone tissue engineering. *Materials Science & Engineering R-Reports*, 80, pp.1–36.
- Yao, X., Peng, R. and Ding, J.D., **2013**. Cell-material interactions revealed via material techniques of surface patterning. *Advanced Materials*, 25(37), pp.5257–5286.
- Lv, L.W., Liu, Y.S., Zhang, P., Gu, M., Bai, X.S., Xiong, C.Y. and Zhou, Y.S., **2018**. Transcriptomics and functional analysis of graphene-guided osteogenic differentiation of mesenchymal stem cells. *Chinese Journal of Dental Research*, 21(2), pp.101–111.
- Kim, S.H., Turnbull, J. and Guimond, S., **2011**. Extracellular matrix and cell signalling: The dynamic cooperation of integrin, proteoglycan and growth factor receptor. *Journal of Endocrinology*, 209(2), pp.139–151.
- Chen, S.C., Guo, Y.L., Liu, R.H., Wu, S.Y., Fang, J.H., Huang, B.X., Li, Z.P., Chen, Z.F. and Chen, Z.T., **2018**. Tuning surface properties of bone biomaterials to manipulate osteoblastic cell adhesion and the signaling pathways for the enhancement of early osseointegration. *Colloids and Surfaces B-Biointerfaces*, 164, pp.58–69.
- Chua, I.L.S., Kim, H.W. and Lee, J.H., **2016**. Signaling of extracellular matrices for tissue regeneration and therapeutics. *Tissue Engineering and Regenerative Medicine*, 13(1), pp.1–12.
- Janson, I.A. and Putnam, A.J., **2015**. Extracellular matrix elasticity and topography: Material-based cues that affect cell function via conserved mechanisms. *Journal of Biomedical Materials Research Part A*, 103(3), pp.1246–1258.
- Morales-Roman, R.M., Guillot-Ferriols, M., Roig-Perez, L., Lanceros-Mendez, S., Gallego-Ferrer, G. and Ribelles, J.L.G., **2019**. Freeze-extraction microporous electroactive supports for cell culture. *European Polymer Journal*, 119, pp.531–540.
- Hsiao, Y.S., Kuo, C.W. and Chen, P.L., **2013**. Multifunctional graphene-PEDOT microelectrodes for on chip manipulation of human mesenchymal stem cells. *Advanced Functional Materials*, 23(37), pp.4649–4656.
- Guillot-Ferriols, M., Rodriguez-Hernandez, J.C., Correia, D.M., Carabineiro, S.A.C., Lanceros-Mendez, S., Ribelles, J.L.G. and Ferrer, G.G., **2020**. Poly(vinylidene) fluoride membranes coated by heparin/collagen layer-by-layer, smart biomimetic approaches for mesenchymal stem cell culture. *Materials Science & Engineering C-Materials for Biological Applications*, 117, pp.1–12.
- Costa, R., Ribeiro, C., Lopes, A.C., Martins, P., Sencadas, V., Soares, R. and Lanceros-Mendez, S., **2013**. Osteoblast, fibroblast and in vivo biological response to poly(vinylidene fluoride) based composite materials. *Journal of Materials Science-Materials in Medicine*, 24(2), pp.395–403.
- Iandolo, D., Ravichandran, A., Liu, X.J., Wen, F., Chan, J.K.Y., Berggren, M., Teoh, S.H. and Simon, D.T., **2016**. Development and characterization of organic electronic scaffolds for bone tissue engineering. *Advanced Healthcare Materials*, 5(12), pp.1505–1512.

30. Luo, W., Chan, E.W.L. and Yousaf, M.N., **2010**. Tailored electroactive and quantitative ligand density microarrays applied to stem cell differentiation. *Journal of the American Chemical Society*, *132*(8), pp.2614–2621.
31. Balikov, D.A., Fang, B., Chun, Y.W., Crowder, S.W., Prasai, D., Lee, J.B., Bolotin, K.I. and Sung, H.J., **2016**. Directing lineage specification of human mesenchymal stem cells by decoupling electrical stimulation and physical patterning on unmodified graphene. *Nanoscale*, *8*(28), pp.13730–13739.
32. Lu, X.Y., Huang, Y., Qu, Y.Y., Zhang, Y.W. and Zhang, Z.Q., **2020**. Integrated transcriptomic and proteomic study on the different molecular mechanisms of PC12 cell growth on chitosan and collagen/chitosan films. *Regenerative Biomaterials*, *7*(6), pp.553–565.
33. Zhao, Y., Fan, T.T., Chen, J.D., Su, J.C., Zhi, X., Pan, P.P., Zou, L. and Zhang, Q.Q., **2019**. Magnetic bioinspired micro/nanostructured composite scaffold for bone regeneration. *Colloids and Surfaces B-Biointerfaces*, *174*, pp.70–79.
34. Lei, X.X., Gao, J.P., Xing, F.Y., Zhang, Y., Ma, Y. and Zhang, G.F., **2019**. Comparative evaluation of the physicochemical properties of nano-hydroxyapatite/collagen and natural bone ceramic/collagen scaffolds and their osteogenesis-promoting effect on MC3T3-e1 cells. *Regenerative Biomaterials*, *6*(6), pp.361–371.
35. Yang, J.R., Xiao, Y.M., Tang, Z.Z., Luo, Z.C., Li, D.X., Wang, Q.G. and Zhang, X.D., **2020**. The negatively charged microenvironment of collagen hydrogels regulates the chondrogenic differentiation of bone marrow mesenchymal stem cells in vitro and in vivo. *Journal of Materials Chemistry B*, *8*(21), pp.4680–4693.
36. Ugarte, G., Santander, C. and Brandan, E., **2010**. Syndecan-4 and beta 1 integrin are regulated by electrical activity in skeletal muscle: Implications for cell adhesion. *Matrix Biology*, *29*(5), pp.383–392.
37. Lee, J.H., Kim, D.H., Lee, H.H. and Kim, H.W., **2019**. Role of nuclear mechanosensitivity in determining cellular responses to forces and biomaterials. *Biomaterials*, *197*, pp.60–71.
38. Ma, D.D., Kou, X.X., Jin, J., Xu, T.T., Wu, M.J., Deng, L.Q., Fu, L.S., Liu, Y., Wu, G. and Lu, H.P., **2016**. Hydrostatic compress force enhances the viability and decreases the apoptosis of condylar chondrocytes through integrin-FAK-ERK/PI3K pathway. *International Journal of Molecular Sciences*, *17*(11), pp.1–15.
39. Kafi, M.A., Aktar, K., Todo, M. and Dahiya, R., **2020**. Engineered chitosan for improved 3D tissue growth through paxillin-FAK-ERK activation. *Regenerative Biomaterials*, *7*(2), pp.141–151.
40. Rittigstein, P., Priestle, R.D., Broadbelt, L.J. and Torkelson, J.M., **2007**. Model polymer nanocomposites provide an understanding of confinement effects in real nanocomposites. *Nature Materials*, *6*(4), pp.278–282.
41. Zhang, X., Shen, Y., Xu, B., Zhang, Q., Gu, L., Jiang, J., Ma, J., Lin, Y. and Nan, C.-W., **2016**. Giant energy density and improved discharge efficiency of solution-processed polymer nanocomposites for dielectric energy storage. *Advanced Materials*, *28*(10), pp.2055–2061.
42. Qiao, K., Guo, S.L., Zheng, Y.D., Xu, X.T., Meng, H.Y., Peng, J., Fang, Z.Y. and Xie, Y.J., **2018**. Effects of graphene on the structure, properties, electro-response behaviors of GO/PAA composite hydrogels and influence of electro-mechanical coupling on BMSC differentiation. *Materials Science & Engineering C-Materials for Biological Applications*, *93*, pp.853–863.
43. Schäfer, C., Borm, B., Born, S., Möhl, C., Eibl, E.-M. and Hoffmann, B., **2009**. One step ahead: Role of filopodia in adhesion formation during cell migration of keratinocytes. *Experimental Cell Research*, *315*(7), pp.1212–1224.
44. Szewczyk, P.K., Metwally, S., Karbownik, J.E., Marzec, M.M., Stodolak-Zych, E., Gruszczynski, A., Bernasik, A. and Stachewicz, U., **2019**. Surface-potential-controlled cell proliferation and collagen mineralization on electrospun polyvinylidene fluoride (PVDF) fiber scaffolds for bone regeneration. *ACS Biomaterials Science & Engineering*, *5*(2), pp.582–593.
45. Sheets, K., Wunsch, S., Ng, C. and Nain, A.S., **2013**. Shape-dependent cell migration and focal adhesion organization on suspended and aligned nanofiber scaffolds. *Acta Biomaterialia*, *9*(7), pp.7169–7177.
46. Sun, Z.Q., Guo, S.S. and Fassler, R., **2016**. Integrin-mediated mechanotransduction. *Journal of Cell Biology*, *215*(4), pp.445–456.
47. Dhavalikar, P., Robinson, A., Lan, Z.Y., Jenkins, D., Chwatko, M., Salhadar, K., Jose, A., Kar, R., Shoga, E., Kannapiran, A. and Cosgriff-Hernandez, E., Review of integrin-targeting biomaterials in tissue engineering. *Advanced Healthcare Materials*, *9*(23), pp.1–26.
48. Yang, C., Tibbitt, M.W., Basta, L. and Anseth, K.S., **2014**. Mechanical memory and dosing influence stem cell fate. *Nature Materials*, *13*(6), pp.645–652.
49. Li, C.J., Xiao, Y., Yang, M., Su, T., Sun, X., Guo, Q., Huang, Y. and Luo, X.H., **2018**. Long noncoding RNA bmncr regulates mesenchymal stem cell fate during skeletal aging. *Journal of Clinical Investigation*, *128*(12), pp.5251–5266.
50. Liu, Y., Zhang, X., Cao, C., Zhang, Y., Wei, J., Li, Y.J., Liang, W., Hu, Z., Zhang, J., Wei, Y. and Deng, X., **2017**. Built-in electric fields dramatically induce enhancement of osseointegration. *Advanced Functional Materials*, *27*(47), pp.1–9.
51. Teixeira, L.N., Crippa, G.E., Gimenes, R., Zaghete, M.A., Deoliveira, P.T., Rosa, A.L. and Beloti, M.M., **2011**. Response of human alveolar bone-derived cells to a novel poly(vinylidene fluoride-trifluoroethylene)/barium titanate membrane. *Journal of Materials Science: Materials in Medicine*, *22*(1), pp.151–158.
52. Gimenes, R., Zaghete, M.A., Bertolini, M., Varela, J.A., Coelho, L.O. and Silva, N.F. **2004**. Composites PVDF-TrFE/BT used as bioactive membranes for enhancing bone regeneration. In *Smart Structures and Materials 2004: Electroactive Polymer Actuators and Devices*, edited by Y. Barcohen, Bellingham, Spie-Int Soc Optical Engineering, pp.539–547.
53. Li, Y., Dai, X., Bai, Y., Liu, Y., Wang, Y., Liu, O., Yan, F., Tang, Z., Zhang, X. and Deng, X., **2017**. Electroactive BaTiO<sub>3</sub> nanoparticle-functionalized fibrous scaffolds enhance osteogenic differentiation of mesenchymal stem cells. *International Journal of Nanomedicine*, *12*, pp.4007–4018.
54. Zhang, C., Liu, W., Cao, C., Zhang, F., Tang, Q., Ma, S., Zhao, J., Hu, L., Shen, Y. and Chen, L., **2018**. Modulating surface potential by controlling the  $\beta$  phase content in poly(vinylidene fluoride-trifluoroethylene) membranes enhances bone regeneration. *Advanced Healthcare Materials*, *7*(11), p.1701466.
55. Wang, C., Lin, K.L., Chang, J. and Sun, J., **2013**. Osteogenesis and angiogenesis induced by porous beta-calcium silicate/PDLGA composite scaffold via activation of AMPK/ERK1/2 and PI3K/Akt pathways. *Biomaterials*, *34*(1), pp.64–77.
56. Gu, H., Guo, F., Zhou, X., Gong, L., Zhang, Y., Zhai, W., Chen, L., Cen, L., Yin, S., Chang, J. and Cui, L., **2011**. The stimulation of osteogenic differentiation of human adipose-derived stem cells by ionic products from akermanite dissolution via activation of the ERK pathway. *Biomaterials*, *32*(29), pp.7023–7033.
57. Yuh, D.Y., Maekawa, T., Li, X., Kajikawa, T., Bdeir, K., Chavakis, T. and Hajishengallis, G., **2020**. The secreted protein DEL-1 activates a beta3 integrin-FAK-ERK1/2-RUNX2 pathway and promotes osteogenic differentiation and bone regeneration. *Journal of Biological Chemistry*, *295*(21), pp.7261–7273.
58. Zhang, B., Li, J., He, L., Huang, H. and Weng, J., **2020**. Bio-surface coated titanium scaffolds with cancellous bone-like biomimetic structure for enhanced bone tissue regeneration. *Acta Biomaterialia*, *114*, pp.431–448.
59. Wang, W., Wang, F., Lu, F., Xu, S., Hu, W., Huang, J., Gu, Q. and Sun, X., **2011**. The antiangiogenic effects of integrin  $\alpha 5\beta 1$  inhibitor (ATN-161) in vitro and in vivo. *Investigative Ophthalmology & Visual Science*, *52*(10), pp.7213–7220.